A Suggested Shape of Spirals for Expanding the Half-Power Beamwidths of UHF Band RFID's Planar Spiral Antennae

Mayumi MATSUNAGA [1], Tsuyoshi MATSUOKA [2], Toshiaki MATSUNAGA [3]
Yasuhiro YOKOTA [1]
[1] Ehime University, 3 Bunkyo-cho, Matsuyama, Ehime 790-8577 Japan
mmayumi@dpc.ehime-u.ac.jp
[2] Kyushu Sangyo University, 2-3-1 Matsukadai Higashi-ku, Fukuoka 813-8503 Japan
tsuyoshi@ieee.org
[3] Fukuoka Institute of Technology, 3-30-1 Wajiro-Higashi, Higashi-ku, Fukuoka 811-0295 Japan
matsunaga@fit.ac.jp

1. Intruduction

A shape of spirals for helping to expand not only the bandwidths but also the half-power beamwidths (HPBW) of UHF band RFID's planar spiral antennae is presented. Considering its application to UHF band's planar spiral antennae utilized as RFID, the antennae are made to radiate fields with wide HPBW, to have wide bandwidth, to be capable of circular polarization, and as small as possible. The UHF band planar spiral antennae equipped with spirals shaped and arranged as per the way introduced in this paper have been found to be capable of radiating fields with HPBW of 120 or more degrees as well as return loss of -10 or less dB within the frequency range between 919 MHz and 966 MHz. This is a performance level far higher than that of conventional planar antennae [1], [2]. The reason for this enhancement of the HPBW and the bandwidth are because the shape of spirals has been formed differently, that is to say the spirals are now arranged like spiralling along outer surface of a cross on a plane without any grands. Therefore, the new antenna has been named "Cross Spiral Antennae (CSA)" after the shape of spirals by the authors. Despite being just changed the shape of the spirals, the HPBW and bandwidths of UHF band RFID's planar antennae have been so greatly expanded while the size of antenna are maintained as same as that of conventional circular polarization antennae of UHF band RFID.

2. The Precise Measurement and Design

In this section, the measurements of the new planar spiral antenna named CSA shall be discussed. First of all, we will discuss the measurements of all the parts of the CSA and explain how those measurements have been determined by using the front and bottom structure of the CSA as in Fig. 1. First, the total length of the innermost loop was set at about 220 mm so as to be a bit smaller than λ of the center frequency of the antenna. The loop was rolled like the shape of the cross as thick as possible and the feed point was set on the loop. Next, the spiral antenna connected at point "A" shown in Fig. 1 and started to spiral the line as thick as possible in same interval. The width of the line and the interval of each line were set at 1 mm. Finally, the line spiralled as thick as possible until the return loss characteristics were got in good condition. Then, the length of each part of the CSA as shown in Fig. 1 were set automatically at L_1= 27 mm, L_2=19 mm, and L_3=28 mm. Therefore, the size of the CSA measured 74 mm by 74 mm. The end point of the spiral referred to "B" was connected to "A" using line located on bottom of the substrate as shown in Fig. 2. Note that, the permittivity of substrate on which the CSA is structured are ε_r=4.8 and tan δ=0.015.

3. Performance Characteristics

First, the return loss frequency characteristics are shown in Fig. 2 to discuss the CSAs' wide bandwidths as well as their low return loss performance levels. The return losses are -10 or less dB within

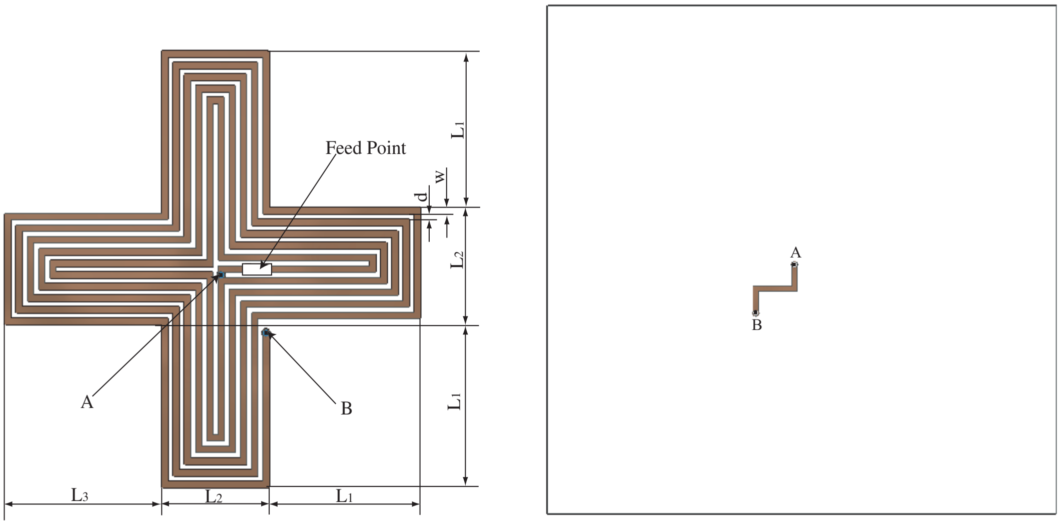

(a)Top view (b)Bottom view

Figure 1: The structure of CSA

the frequency range between 919 MHz and 966 MHz. Therefore, the bandwidth of the CSA being 47 or more MHz, the CSA may well be looked upon as good wide-band antennae. The results of the measurement of the return loss are shown in Fig. 2(b). Although the frequency range in which the return losses of the CSA are -10 or less dB is a bit shifted to upper frequencies, the fact that the CSA is capable of wide bandwidth as well as its low return loss performance has been verified. Next, the results of the measurement of the radiation field patterns of the CSA are shown in Fig. 3. Figure 3 shows, with solid blue lines, the measurement of the radiation field patterns in the E-plane and the H-plane at 950 MHz. This figure gives numerical results obtained by numerical analysis as well, plotted as dashed black lines. The measurement data show that the HPBW is 120 or more degrees in the E-plane and almost 180 degrees in the H-plane, and that these results are similar to those of numerical analyses. Then, the co-polarized and cross-polarized radiation field patterns occurring when the CSA is used at 950 MHz are shown in Fig. 4. From the results given in figure 4, it is apparent that the CSA can send/receive radiation fields when the direction of polarization is mismatched between sender and receiver. Finally, the right-hand polarization and left-hand polarization patterns are shown in Fig. 5. From the results, it is apparent that the CSA presented in this paper radiates right-hand polarization as well as separates enough left-hand polarization.

4. Conclusion

A new arrangement of the spirals of planar spiral antennae has made it possible to greatly improve the HPBW and bandwidth performance of the UHF band RFID antennae. The arrangement and shape of spirals being so simply changed that the line in same width spirals like winding along the outer side of a cross continuously in same interval on a plane, the HPBW and bandwidths of the planar spiral antennae, that are to be used in UHF band RFID antennae wherein such an improvement has long been extremely difficult, have been vastly expanded. The performances of the planar spiral antennae set forth in this paper have been done for the verification not only by way of numerical analyses but also by way of experiment. According to the numerical results of return loss and antennae beam pattern obtained by experimental measurements and numerical analyses, the wide HPBW and bandwidth of the CSA are verified. Those demonstrate the effectiveness of the new arrangement of spirals and will provide an effective way of developing UHF band RFID's planar antennae highly efficient with low communication errors.

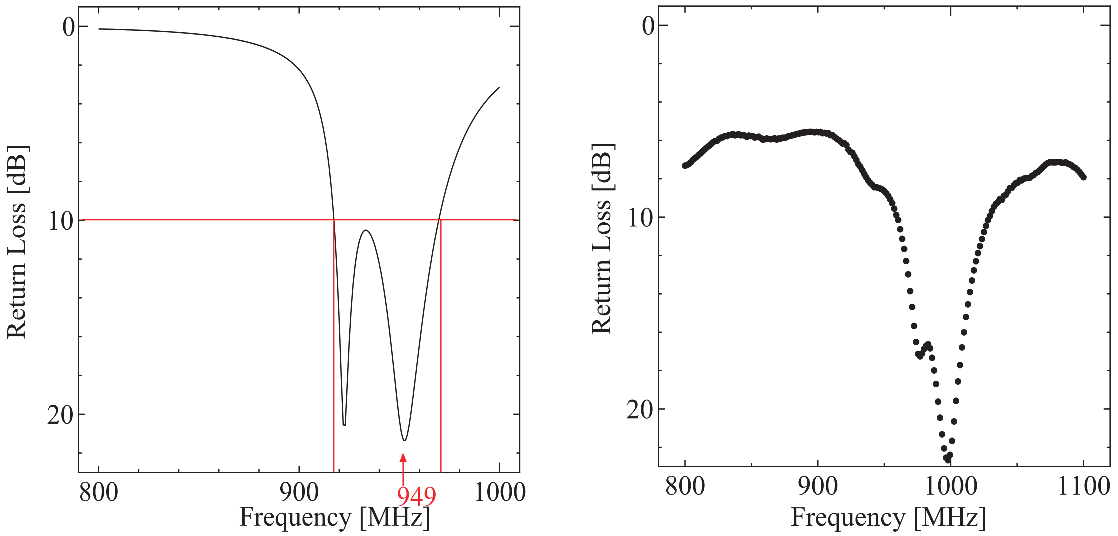

(a)Results of Numerical analyses (b)Results of experimental measurements

Figure 2: Return loss characteristis of the CSA

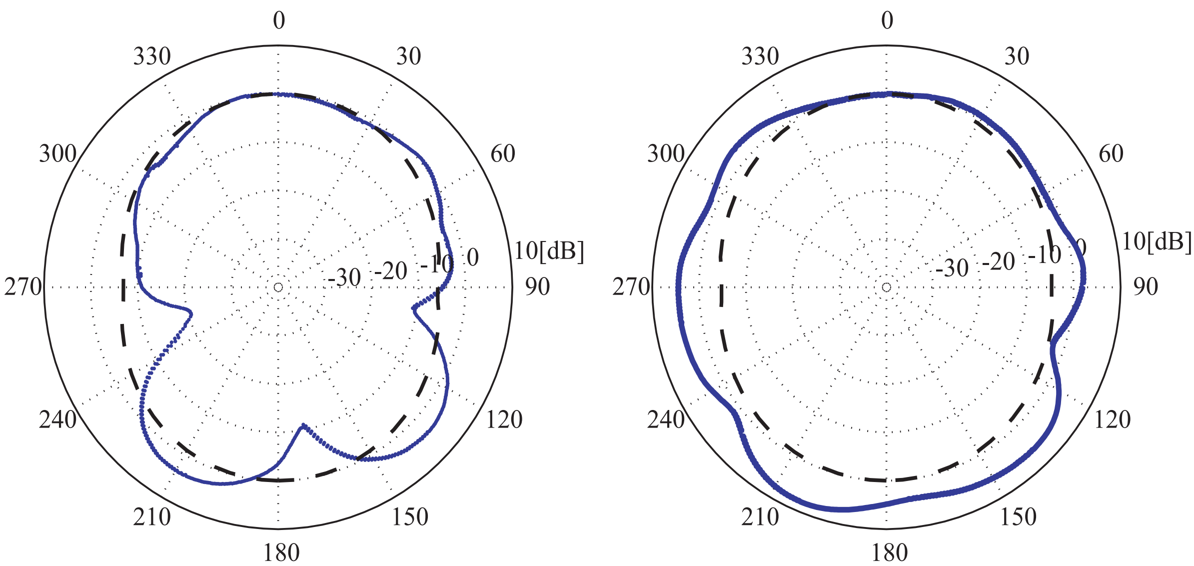

(a) E-plane (b) H-plane

Figure 3: Radiation field patterns occurring on the E- and H-planes when the CSA is used at 950 MHz are shown in (a) and (b), respectively. The dashed black lines refer to the numerical data, the solid blue lines refer to the measured data.

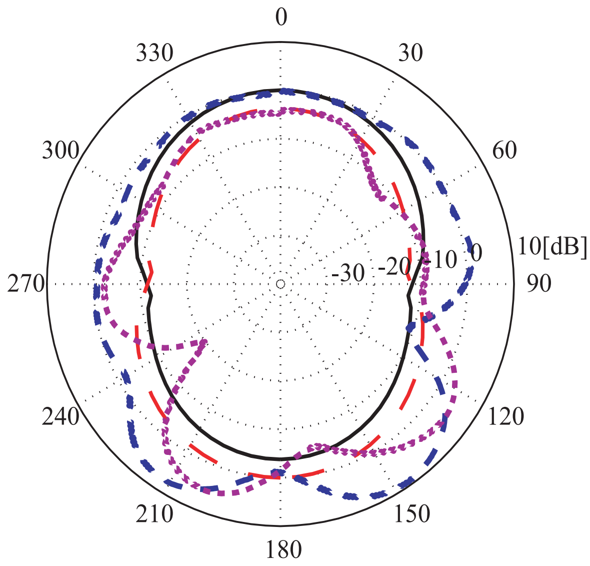

Figure 4: The co-polarized and the cross-polarized radiation field patterns occurring in the ϕ = 45 degree plane when the CSA is used at 950 MHz are shown. The solid black line refers to the co-polarized field and the dashed red line refers to the cross-polarized field, which are obtained by numerical analyses. The short dashed blue line refer to the co-polarized field and the solid violet lines refer to the cross-polarized field, which are obtained by experimental measurements.

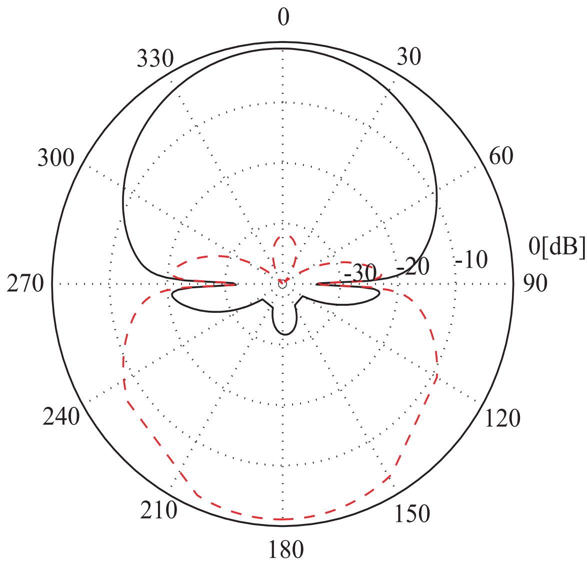

Figure 5: The right-hand polarization and the left-hand polarization patterns when the CSA is used at 950 MHz is shown. The solid black line refers to the right-hand polarization and the dashed red line refers to the left-hand polarization, which are obtained by numerical analyses.

Acknowledgments

The authors gratefully acknowledge the assistance of the Ministry of Internal Affairs and Communications of Japan and the Japan Science and Technology Agency for their support by way of the Strategic Information and Communications R&D Promotion Programme (SCOPE) and the Project to develop “innovative seeds”, respectively.

References

[1] C. A. Balanis, *Antenna Theory*, 3-rd edition, John Wiley and Sons, New Jersey, pp.611–652, 811–882, 2005.

[2] W. L. Stutzman, G. A. Thiele, *Antenna Theory and Design*, 2-nd edition, John Wiley and Sons, New York, pp.225–270, 1998.